SAND2013-10606C

Effect of Ignition Improvers on the Combustion Performance of Regular Gasoline in an HCCI Engine

Chunsheng Ji, John E. Dec, Jeremie Dernotte
Sandia National Laboratories

William Cannella
Chevron USA, Inc.

Abstract

This study explores the use of two conventional ignition improvers, 2-ethylhexyl nitrate (EHN) and di-tert-butyl peroxide (DTBP), to enhance the autoignition of the regular gasoline in an homogeneous charge compression ignition (HCCI) engine at naturally aspirated and moderately boosted conditions (up to 180 kPa absolute) with a constant engine speed of 1200 rpm. The results showed that both EHN and DTBP are very effective for reducing the intake temperature (T_{in}) required for autoignition and for enhancing stability to allow a higher charge-mass fuel/air equivalence ratio (ϕ_m). On the other hand, the addition of these additives can also make the gasoline too reactive at some conditions, so significant exhaust gas recirculation (EGR) is required at these conditions to maintain the desired combustion phasing. Thus, there is a trade-off between improving stability and reducing the oxygen available for combustion when using ignition improvers to extend the high-load limit. Because previous works have shown that partial fuel stratification (PFS) can be applied with more reactive fuels to reduce the heat release rate to allow higher loads or more advanced combustion timing without knock, the potential of the ignition improvers to allow effective PFS was also explored over the same range of intake pressures. The effect of the additives on NOx emissions was also studied. The results showed that NOx emissions increase with increased EHN concentration but are not affected by DTBP. This work indicates that conventional ignition improvers can effectively enhance the HCCI autoignition reactivity of conventional gasoline at naturally aspirated and modestly boosted operations, offering significant benefits for HCCI engines.

Keywords

HCCI; Autoignition Reactivity; Ignition Improvers; ITHR; PFS

Introduction

Homogeneous charge compression ignition (HCCI) sometimes called controlled auto ignition (CAI) engines are considered as an alternative to conventional Spark Ignition (SI) and Compression Ignition (CI) engines. The HCCI combustion process is well known to provide much lower NOx and particulate matter emissions compared with conventional engines. Meanwhile, the HCCI engines can have a 30% improvement in thermal efficiency compared with SI engines, which is typically comparable to diesel engines with similar displacement. Recent studies [1-3] have further revealed that the thermal efficiencies of HCCI engines can be further improved by applying Partial Fuel Stratification (PFS) in combination with intake boost.

However, significant challenges still remain to be solved with HCCI engines before their widespread application. One significant challenge for HCCI is to control the ignition timing. Unlike conventional engines in which the ignition is either controlled by using a spark (SI combustion) or by controlling the fuel injection (diesel or conventional CI combustion), the ignition in HCCI is controlled by chemical kinetics, which are sensitive to many factors including fuel properties, oxygen and exhaust gas recirculation (EGR) concentration, temperature, and pressure. For example, although HCCI engines can operate on regular gasoline at naturally aspirated conditions, a large amount of hot residuals or a high intake temperature is necessary for autoignition due to gasoline's low HCCI autoignition reactivity [4]. As a result, charge densities are much lower than those of typical engines, which is an important factor limiting the loads of HCCI engines. Previous work [3] has shown that these problems can be substantially reduced by the use of a low-octane gasoline. Moreover, the combustion phasing for a more reactive fuel can be retarded farther with good stability, which allows higher charge-mass fuel/air equivalence ratio (ϕ_m) without knock. The combination of higher ϕ_m and higher charge density with low-octane fuels has been shown to have the potential to significantly increase the load limit compared to regular gasoline. Although low-octane gasoline has shown to be more suitable for HCCI engines compared with conventional gasoline at naturally aspirated condition, these fuels are not readily available in the market. Additionally, the high reactivity of low-octane gasoline can turn into a hindrance for intake-boosted operation above a particular boost level. This is because the fuel/air mixture becomes so reactive that a large amount of EGR is required to prevent serious knock. Under such circumstances, the maximum load can become limited by a lack of oxygen [3].

To find an ideal fuel for HCCI engines, a number of studies have been conducted to investigate the effect of fuel type on the HCCI performance [e.g., 3-13]. To overcome the low reactivity of conventional gasoline, mixtures of primary reference fuels (PRF) with octane numbers (ON) lower than regular gasoline's are also commonly used in the studies of HCCI engines [e.g., 14-16]. Alternatively, some conventional ignition improvers, such as 2-ethylhexyl nitrate (EHN) and di-tert-butyl peroxide (DTBP) which are used to improve the cetane number (CN) of diesel fuels, have attracted researchers' interests as a means to enhance the autoignition of regular gasoline in HCCI engines. Both EHN and DTBP have shown to improve the CN of diesel fuel effectively by using a very small amount (<1% by vol.) as reported by the EPA [17]. Similar effects of these additives on the enhancement of autoignition have also been found in the HCCI engines. Reitz and co-workers [18, 19] found that EHN can enhance the autoignition reactivity of low reactivity fuels such as gasoline and E10 (i.e., 10% ethanol in gasoline). Hosseini et al. [20] indicated that a small amount of EHN additive advanced low temperature heat release (LTHR) and high EGR rates were required to retard the combustion phasing. Eng et al. [21] showed that adding DTBP to a fully-blended gasoline both advances the location of maximum energy release and lowers the minimum fueling level for stable HCCI combustion at low loads. They also found that the effect of DTBP in reducing the minimum fueling level was nonlinear. More specifically, DTBP addition levels up to 2% produced a large change in ignition timing, while adding greater amounts resulted in only a small change in ignition timing. Mack et al. [22] observed that with the addition of DTBP, a lower inlet temperature was required but it didn't make later combustion timings easier to obtain. Moreover, the addition of DTBP was found to have different effects on different fuel types. Cernansky and co-workers [23] also indicated that the effect of DTBP is primarily chemical for high ON PRF blends but thermal for low ON PRF blends. Subsequently, authors from the same research group further numerically studied the effect of DTBP on PRF fuels. They [24] concluded that the addition of DTBP amplifies the LTHR and reduces the ON.

Despite the lower cost and greater enhancement in CN of EHN compared with DTBP, there is a concern that the nitrate group in EHN may increase the NOx emissions. Thompson et al. [25] have shown that the addition of EHN has almost no effect on NOx emissions in conventional diesel operation. However, the EHN doped fuels have been found to increase the NOx emissions in low-temperature diesel combustion as reported by Ickes et al. [26] and Bunting et al. [27]. More specifically, Ickes et al. [26] indicated that 30% of the nitrate group in EHN tends to convert to NOx and the NOx emissions increase proportionally with the amount of EHN. Reitz and co-workers [18, 19] reported that the nitrogen in EHN results in a small increase in NOx emissions from the light-duty reactivity controlled compression ignition (RCCI) combustion. Hosseini et al. [20] showed that EHN produced higher NOx emissions on a relative basis, but the absolute emissions were still low. Comparatively, DTBP was shown to have either minor or no detectable effects on NOx emissions [28].

In summary, the previous works show that the conventional ignition improvers can enhance the autoignition of the regular gasoline in HCCI engines with the potential for a small increase in NOx emissions for EHN. However, there is a dearth of information on understanding the effects of such additives on the operating limits at different boost levels. The effects of conventional ignition improvers on the HCCI operation need to be further validated and understood over a wide range of conditions.

The objective of the current work is to examine the potential for using conventional ignition improvers to enhance the autoignition of regular gasoline in an HCCI engine at naturally aspirated and moderately boosted conditions (up to 180 kPa absolute). The effects of EHN and DTBP on the high-load limit at each intake pressure (P_{in}) were studied and compared. Additionally, because previous works have shown that PFS can be applied with more reactive fuels to reduce the heat release rate to allow higher loads or more advanced combustion timing without knock [3, 29, 30], the potential of the ignition improvers to allow effective PFS was also explored over the same range of intake pressure. Finally, the effect of the additives on NOx emissions was investigated.

The next section describes the experimental facility, data acquisition and analysis techniques, fuel/additive properties, and test conditions. Following this, the results are presented in four parts. First, the effects of EHN and DTBP on the autoignition enhancement of regular gasoline in the HCCI engine are presented and discussed. The second part shows that the high-load limits at various P_{in}'s are strongly dependent on the additive concentration. The third part further reveals the potential of PFS to improve the thermal efficiency for the additized fuels. The last part compares the NOx emissions between the base fuel and additized fuels. Finally, the present work is summarized, and conclusions are drawn in the last section.

Experimental Setup

Engine Facility

The HCCI research engine used for this study was derived from a Cummins B-series six-cylinder diesel engine, which is a typical medium-duty diesel engine with a displacement of 0.98 liters/cylinder. As shown in Fig. 1a, the engine has been converted for single-cylinder operation by deactivating cylinders 1-5. The active HCCI cylinder is fitted with a compression-ratio (CR) = 14 custom piston as shown in Fig. 1b. This piston provides an open combustion chamber with a large squish clearance and a quasi-hemispherical bowl. The engine specifications and operating conditions are listed in Table 1. The configuration of the engine and facility are identical to those used in our previous studies of gasoline [2, 4] and low-octane fuels [3, 29, 30].

A combination of premixed and direct injection (DI) fueling was used as shown in Fig. 1. The premixed fueling system, shown at the top of the schematic in Fig. 1a, consists of a gasoline direct injection (GDI) fuel injector mounted in an electrically heated fuel-vaporizing chamber and appropriate plumbing to ensure thorough premixing with the air and EGR upstream of the intake plenum. The DI fueling is accomplished using a second GDI injector mounted centrally in the cylinder head. A positive displacement fuel flow meter was used to determine the amount of fuel supplied.

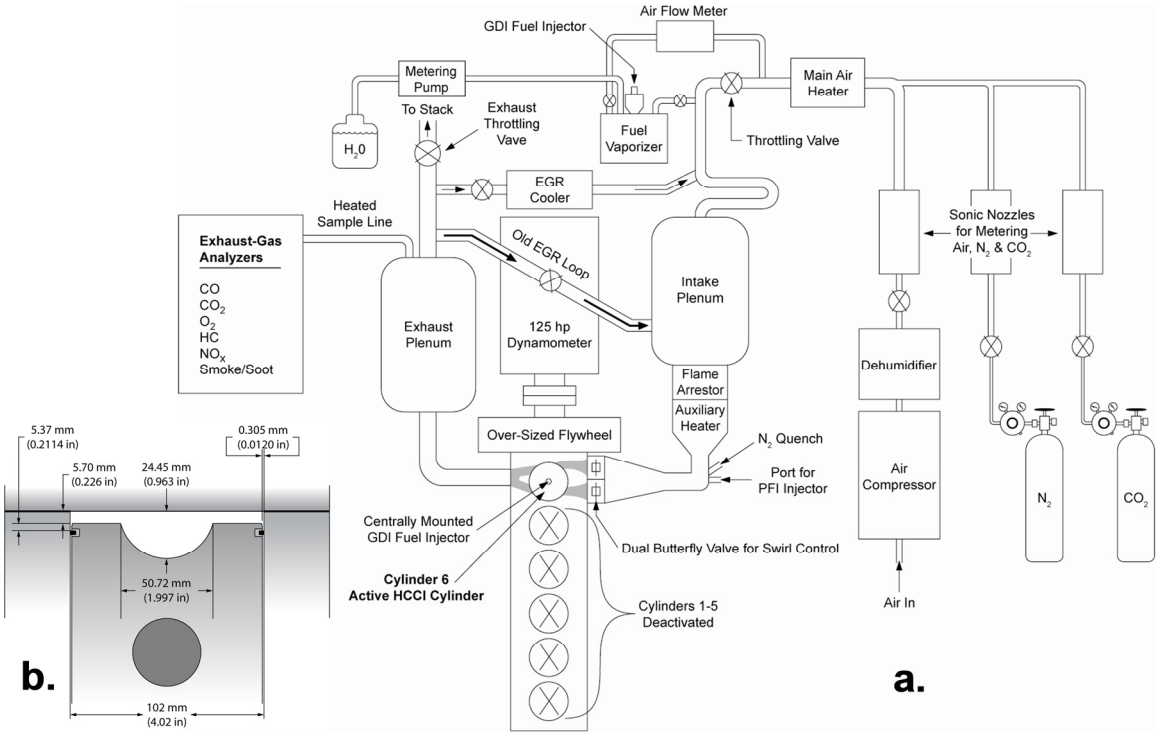

Figure 1. Schematic of HCCI engine facility (a) and combustion chamber geometry of the CR = 14 piston, at TDC (b).

Table 1. Engine specifications and operating conditions.

Displacement (single-cylinder)	0.981 liters
Bore	102 mm
Stroke	120 mm
Connecting Rod Length	192 mm
Geometric Compression Ratio	14:1
Number of Valves	4
IVO	0° CA*
IVC	202° CA*
EVO	482° CA*
EVC	8° CA*
Swirl Ratio	0.9
Fueling system	Fully Premixed/GD
DI Injector	Bosch, 8-hole
Included Angle	70°
Hole Size (Stepped-hole)	min. dia. = 0.125 mm
Max. Injection Pressure	135 bar
Engine Speed	1200 rpm
Intake Pressure (abs.)	100 ~ 180 kPa
Intake Temperature	60 ~ 145°C
Coolant/Oil Temperature	100°C

* 0° CA is taken to be TDC intake. The valve-event timings correspond to 0.1 mm lift.

The intake air was supplied by an air compressor and precisely metered by a sonic nozzle. Both real and simulated EGR were used in this work. The cooled real EGR is introduced well upstream of the intake plenum to ensure that the intake charge is well mixed. The exhaust pressure is controlled by throttling the exhaust flow so that it is higher than the intake pressure (typically 1~3 kPa in this work), which allows the EGR to flow back into the intake. Simulated EGR consisting of N_2 and CO_2 was also used in this work for some measurements where the amount of combustion products needs to be carefully controlled. Unlike the complete stoichiometric products (or CSP) used for EGR simulation in some previous works from our laboratory [e.g., 3, 4], the simulated EGR used in the current work did not include H_2O. In order to compensate for this, the amounts of N_2 and CO_2 were adjusted to provide the same total moles and the same specific heat capacity (c_p) as CSP containing H_2O. The amounts of N_2 and CO_2 were precisely controlled using sonic nozzles as indicated in Fig. 1a. This simulated EGR is hereafter called CSPd standing for dry CSP.

An equivalence ratio based on the total charge-mass, rather than air alone, is used in the current work. This equivalence ratio, referred to as charge-mass equivalence ratio (ϕ_m) is defined as

$$\phi_m = \frac{(F/C)}{(F/A)_{stoich}} \quad (1)$$

where *F/C* is the mass ratio of fuel and total inducted charge gas (*i.e.* fresh air and EGR or CSPd), and $(F/A)_{stoich}$ is the mass ratio of stoichiometric fuel/air mixture for complete combustion. This provides a convenient and consistent way to compare data with the same supplied energy content per unit charge mass (*i.e.*, the same dilution level) for operating conditions with different fuels and different EGR levels. Note that ϕ_m is the same as conventional air-based ϕ when no EGR/CSPd is used. It should also be noted that the air-based

ϕ is ≤ 1 for all conditions presented, so combustion is never fuel rich overall.

The intake pressures varied from 100 kPa (simulating naturally aspirated conditions) to 180 kPa for the current study. All pressures given are absolute. The engine was fully preheated and kept at 100°C during all the tests by means of electrical heaters on the cooling water and lubricating-oil circulation systems. In addition, the intake tank and plumbing were preheated to 50 - 60°C to avoid condensation of the fuel or water from the EGR gases. An auxiliary heater mounted close to the engine provided precise control of the intake temperature to maintain the desired combustion phasing. Intake temperatures ranged from 60° - 145°C. All data were taken at an engine speed of 1200 rpm.

Data Acquisition

Cylinder pressure was measured with a transducer (AVL QC33C) mounted in the cylinder head approximately 42 mm off center. The pressure transducer signals were digitized and recorded at 0.25° Crank Angle (CA) increments for one hundred consecutive cycles. The cylinder-pressure transducer was pegged to the intake pressure near bottom dead center (BDC) where the cylinder pressure reading was virtually constant for several degrees. Intake temperatures were monitored using *K*-type thermocouples mounted in the two intake runners close to the cylinder head. Firedeck temperatures were monitored with a *K*-type thermocouple embedded in the cylinder head so that its junction was about 44 mm off the cylinder center and 2.5 mm beneath the surface. Surface temperatures were estimated by extrapolating the thermocouple reading to the surface, using the thickness of the firedeck and assuming that its back surface was at the 100°C cooling-water temperature [29]. For all data presented, 0°CA is defined as TDC (top dead center) intake (so TDC compression is at 360°CA). This eliminates the need to use negative crank angles or combined bTDC, aTDC notation.

The crank angle of the 50% burn point (CA50) was used to monitor the combustion phasing, and the 10% burn point (CA10) was used as a representative marker for the hot-ignition point. CA10 and CA50 were determined from the cumulative apparent heat-release rate (AHRR), computed from the cylinder-pressure data (after applying a 2.5 kHz low-pass filter [3130]). The start of heat release is set at the minimum point on the AHRR curve before the main heat release peak. For two-stage ignition cases, this minimum point is located between the LTHR peak and main heat release peak. This method provides a consistent measure to compare CA10 and CA50 of main combustion event although LTHR is excluded from burn-duration calculation. Computations of CA10 and CA50 were performed for each individual cycle, disregarding heat transfer and assuming a constant ratio of specific heats ($\gamma = c_p/c_v$) [32]. The average of 100 consecutive individual-cycle CA10 or CA50 values were then used to monitor CA10 or CA50 during operation and for the values reported. The reported pressure rise rates (PRRs) and ringing intensities (see Eq. 2) are computed from the same low-pass-filtered pressure data. For each cycle, the maximum PRR was analyzed separately with a linear fit over a moving ±0.5° CA window. Similar to CA50, these individual-cycle values were then averaged over the 100-cycle data set.

The acceptable knock limit for HCCI engines is often defined in terms of a maximum allowable PRR ($dP/d\theta$, where θ is a variable representing °CA). However, this does not correctly reflect the potential for knock under boosted conditions where the cylinder pressure changes significantly. In this work, the correlation for ringing intensity developed by Eng [33] is used as a measure of engine knock:

$$\text{Ringing Intensity} \approx \frac{1}{2\gamma} \cdot \frac{\left(0.05 \cdot \left(\frac{dP}{dt}\right)_{max}\right)^2}{P_{max}} \cdot \sqrt{\gamma R T_{max}} \quad (2)$$

where $(dP/dt)_{max}$, P_{max}, and T_{max} are the maximum values of PRR (in real time), pressure, and temperature, respectively, γ is the ratio of specific heats, and R is the gas constant. Based on the onset of an audible knocking sound and the appearance of obvious ripples on the pressure trace, a ringing criterion of 5 MW/m^2 was selected as the ringing limit for operation without knock. This corresponds to about 8 bar/°CA at 1200 rpm at naturally aspirated for operating conditions typical of those used in this study. At all boost levels tested, perceived engine knock correlated well with the ringing intensity rising above 5 MW/m^2, giving confidence in this correlation.

A second method of computing the heat-release rate (HRR) was used for detailed HRR-curve analysis. Here, the heat release was computed in a more refined way from the ensemble-averaged pressure trace (with the 2.5 kHz low-pass filter applied), using the Woschni correlation for heat transfer [32]. The results of this detailed HRR analysis are mainly used for comparisons of the early part of the heat release, leading up to hot ignition.

Exhaust emissions data were also acquired, with the sample being drawn just downstream of the exhaust plenum using a heated sample line (See Fig. 1a). CO, CO_2, HC, NOx, and O_2 levels were measured using standard exhaust-gas analysis equipment as used in our previous studies [e.g., 34]. In addition, a second CO_2 meter monitored the intake gases just prior to induction into the engine, which allowed the EGR fraction of the intake gases to be computed from the ratio of the intake and exhaust CO_2 concentrations.

Fuel/Additives Properties and Test Conditions

A regular Chevron commercial gasoline containing 10 vol.% ethanol (supplied by Chevron), hereafter referred as CCG-E10, is used in the current study. Table 2 lists the fuel properties of this fuel. Multiple batches of fuels were used in this work and the batch-to-batch variation was found negligible. Compared with the research-grade conventional gasoline with no ethanol (Antiknock Index, AKI=87) used in our previous studies [1, 2, 4], CCG-E10 shows higher RON and MON.

EHN with a purity of 97% and DTBP with a purity of 95% are used in the current work (most of the impurities are isomers). The additives were mixed well with CCG-E10 on a volume percentage basis, and the physical properties of fuel mixtures were calculated carefully based on the known specifications of CCG-E10 and additives.

Table 2. Fuel properties of CCG-E10.

Formula	$C_{5.76}H_{11.98}O_{0.22}$
Specific gravity (15 °C)	0.7238
Net Heating Value, MJ/kg	41.74
Carbon, wt, %	81.67
Hydrogen, wt, %	4.06
RON	92.5
MON	84.6
Antiknock Index (R+M)/2	88.6

The effect of EHN and DTBP addition on the CN improvement is shown in Fig. 2. Both additives are shown to effectively increase CN of CCG-E10. The improvement however is nonlinear for both additives. A greater increase in CN is found for a low percentage of additive (<0.25 vol.%), and the effect becomes more moderate and nearly linear over the range of 0.25-1.0 vol.% additive. Furthermore, EHN displays a greater increase in CN for a given additive percentage than DTBP does, over the whole range tested.

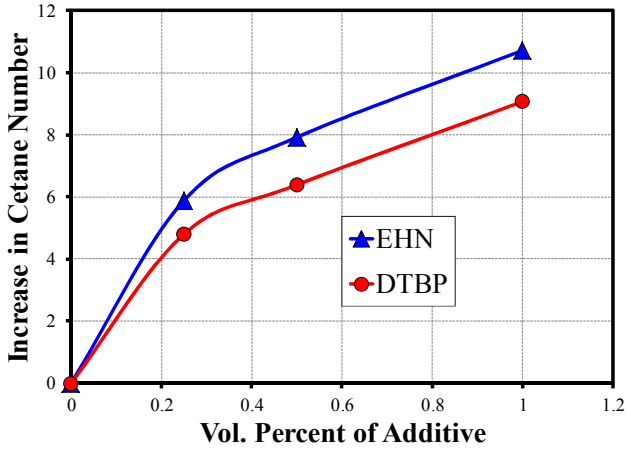

Figure 2. Cetane improvement of CCG-E10 using EHN and DTBP.

For each condition tested, the high-load limit was approached by first operating the engine at a relatively stable condition, and then gradually increasing the fueling rate to either the knock/stability limit or oxygen/stoichiometric limit (these terms will be defined later in the section on high-load limits), whichever came first. During this process, constant ringing intensity, 5 MW/m^2, was used in most cases. However, lower ringing intensities (~3 MW/m^2) were used in several cases where it produced a more stable combustion phasing. Previous studies [1, 4] have revealed that fuels with high autoignition reactivity show stronger intermediate temperature heat release (ITHR) which occurs after the LTHR and leads into the hot ignition (see Fig. 5 for detailed illustration of LTHR and ITHR). Thus, a separate set of experiments was performed to investigate the variation of ITHR at various P_{in}'s and additive concentrations. For this sweep, ϕ_m was held constant and the CA10 was kept constant by varying EGR or intake temperature (T_{in}).

To obtain the benefits of PFS, the fuel must be "ϕ-sensitive" so that autoignition occurs sequentially from richer to leaner regions [6, 29,30]. Strong ϕ-sensitivity means that the autoignition timing of a fuel is strongly dependent on ϕ_m, i.e., the zones with high ϕ_m autoignite sooner and low-ϕ_m zones autoignite later. Because of this effect, mixture stratification is effective for slowing down the combustion process for ϕ-sensitive fuels [35]. A ϕ-sensitivity test of the additized fuel was conducted before applying PFS. For this test, an alternative firing method was used in order to isolate the fuel-chemistry effect that produced ϕ-sensitivity from thermal and residual-gas effects on ignition timing as ϕ_m is varied [6]. Similar methodology has also been used and validated in previous studies [e.g., 1, 30, 35]

Throughout the current work, care was taken to make sure that the data were collected under conditions where the HCCI combustion was clean (NOx < 0.1 g/kWh, near-zero soot), complete (combustion efficiency > 95%), stable (COV of $IMEP_g$ ≤ 1%), and not knocking (ringing intensity ≤ 5 MW/m^2), unless otherwise noted.

Results and Discussion

HCCI Autoignition Reactivity

HCCI combustion is extremely sensitive to initial thermodynamic conditions. Usually high T_{in} (~140°C) is required for fuels with low HCCI reactivity, such as regular gasoline and E10 [2] at naturally aspirated conditions. A lower T_{in} can be achieved by either increasing the intake pressure [1] or using a more reactive fuel such as hydrobate [3]. Both methods enhance the rate of chemical reactions in the early stages before the hot ignition, reducing the required T_{in}. Thus, it is of great interest to find out whether adding EHN and DTBP to the CCG-E10 can affect the required T_{in} in a manner similar to a high-reactivity fuel. Figure 3 shows the effect of EHN and DTBP addition to the CCG-E10 fuel on the T_{in} required to maintain the same CA10 (366.3°CA) for a constant ϕ_m = 0.4 at P_{in} = 100 kPa. By adding small amount of EHN (0.15%) or DTBP (0.35%), the T_{in} drops drastically from 144°C to 95°C. T_{in} can be further reduced to 60°C using 0.4%EHN (Fig. 3).

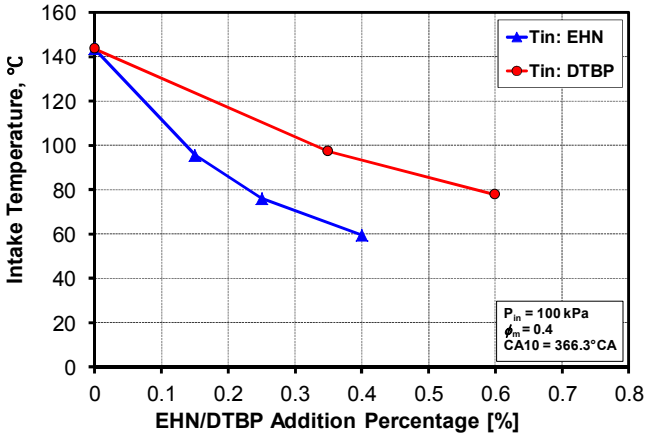

Figure 3. Effect of EHN and DTBP addition on intake temperature (T_{in}) at naturally aspirated conditions (P_{in}= 100 kPa), ϕ_m = 0.4, and CA10 = 366.3°CA.

Compared with EHN, DTBP has a smaller effect on T_{in} for a given percentage added as shown in Fig. 3. Moreover, a nonlinear decrease in T_{in} is found for both EHN and DTBP; the decrease of T_{in} is shown to be greater at low additive concentration (<0.25%) and the effect becomes more moderate as the additive percentage increases. The observations are consistent with those for the CN increase with additive concentration (Fig. 2).

As shown in Fig. 3, more than double the amount of DTBP is required to achieve the same effect as EHN, at least for the test fuel and test range studied in the present work. To further illustrate this point, P_{in} and ϕ_m are varied for the cases of 0.25%EHN and 0.6% DTBP (which require nearly the same T_{in}) to compare their effects on HCCI combustion. The results are shown in Fig. 4.

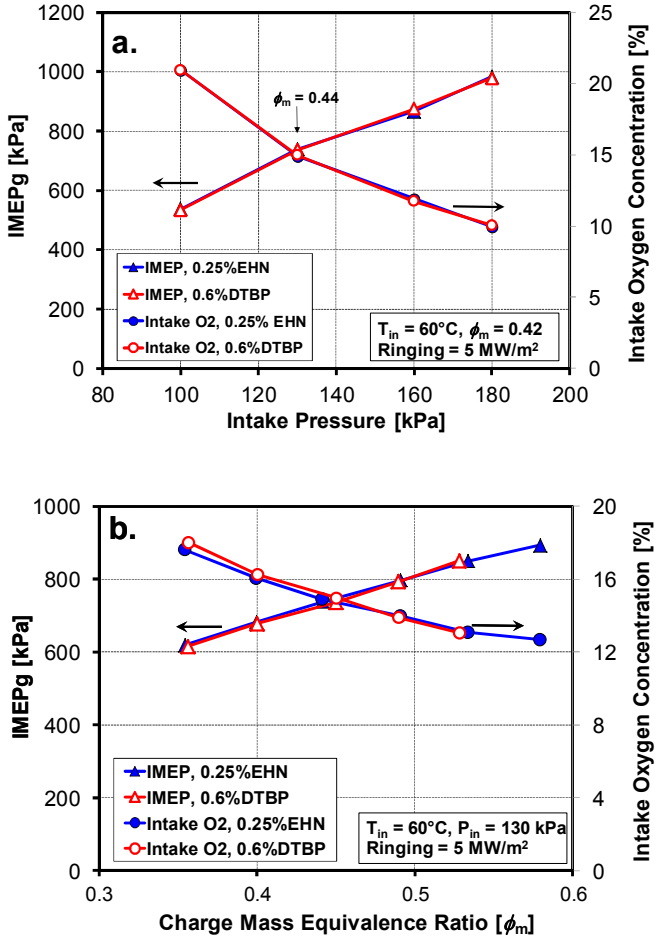

Figure 4. Gross indicated mean effective pressure ($IMEP_g$) and intake oxygen concentration at various P_{in} (a) and ϕ_m (b) for 0.25%EHN and 0.6%DTBP fuel mixture. For Fig. 4a, ϕ_m = 0.42 at all P_{in}'s except for P_{in}= 130 kPa where ϕ_m = 0.44. In all the results shown above, T_{in} was kept constant at 60°C and ringing intensity = 5 MW/m^2. EGR was used to adjust CA50 to keep the same ringing.

Fig. 4a shows that 0.25%EHN and 0.6%DTBP have nearly identical gross indicated mean effective pressure ($IMEP_g$) and intake oxygen concentration over a range of P_{in}'s from 100 kPa to 180 kPa at otherwise similar conditions. It should be noted that the increase of P_{in} enhances the autoignition reactivity, which requires more EGR to delay the autoignition timing sufficiently to prevent knocking and keep the same ringing (5 MW/m^2). Thus, a decrease in intake oxygen concentration was observed as P_{in} was increased from 100 kPa to 180 kPa. In Fig. 4b, the IMEPg and intake O_2 for both 0.25%EHN and 0.6%DTBP are also plotted as a function of ϕ_m at constant P_{in} and T_{in}. As can be seen, increasing ϕ_m causes a nearly identical increase in the IMEPg and a reduction in intake O_2 for both 0.25%EHN and 0.6%DTBP, similar to the effect of increasing P_{in} (Fig. 4a). Since the purpose of Fig. 4b is to show the consistency between the 0.25%EHN and 0.6%DTBP additized fuels, the 0.6%DTBP dataset was not fully extended to the highest possible load, as was done for 0.25%EHN.

Although the HCCI reactivity enhancement by EHN and DTBP is similar to their effect on CN as shown in Fig. 2, the CN may not be an ideal index for HCCI reactivity. For example, despite the fact that 0.25%EHN and 0.6%DTBP mixtures show nearly identical HCCI reactivity, the increase of CN is different for these two mixtures, being around 7 for 0.6%DTBP and 6 for 0.25%EHN as shown in Fig. 2. In other words, fuels with same CN may show different HCCI combustion characteristics. This conclusion is consistent with that reported by Hosseini et al. [20].

As discussed above, the HCCI autoignition reactivity of CCG-E10 is significantly enhanced by adding a small amount of EHN and DTBP. Consequently, the ITHR should be also enhanced as reported in previous studies [29, 30]. For a clear illustration of LTHR, ITHR and main heat release, a normalized HRR profile for CCG-E10 with 0.4%EHN mixture is plotted in Fig. 5.

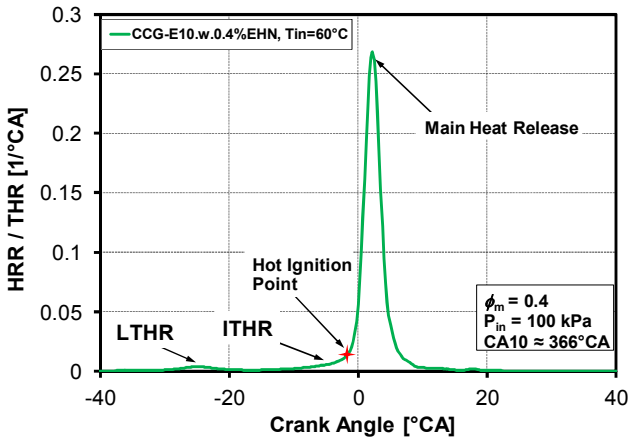

Figure 5. Normalized HRR profile for a CCG-E10 with 0.4%EHN mixture at P_{in} = 100 kPa, ϕ_m = 0.4 and CA10 ≈ 366°CA.

In order to better understand the effect of EHN and DTBP on the ITHR enhancement, enlarged plots of the HRR just before hot ignition are shown in Fig. 6a for fuels with various amounts of additive. For these data, T_{in} was adjusted with changes in additive concentration to maintain CA10 ≈ 366°CA (constant P_{in} = 100 kPa and ϕ_m = 0.4). The HRR profiles have been normalized by the total amount of detected heat release (THR) in order to eliminate differences between HRR profiles caused solely by a difference in the total amount of fuel injected per cycle as T_{in} is varied. The ITHR of a research-grade

conventional gasoline with no ethanol [1, 2, 4] (AKI = 87) that has similar HCCI reactivity to CCG-E10 is also plotted for comparison purposes. As shown in Fig. 6a, the CCG-E10 without any additives shows a weak ITHR, which is very similar to the conventional gasoline used in our previous studies [3, 4]. However, by adding 0.15%EHN or 0.35%DTBP to the CCG-E10 gasoline, the ITHR increases significantly and the enhancement of ITHR increases with increasing additive concentration. The LTHR is also enhanced with increased additive concentration, with the amount of LTHR being approximately proportional to the additive concentration. It is also found that the timing of the LTHR peak is retarded with increasing additive contents.

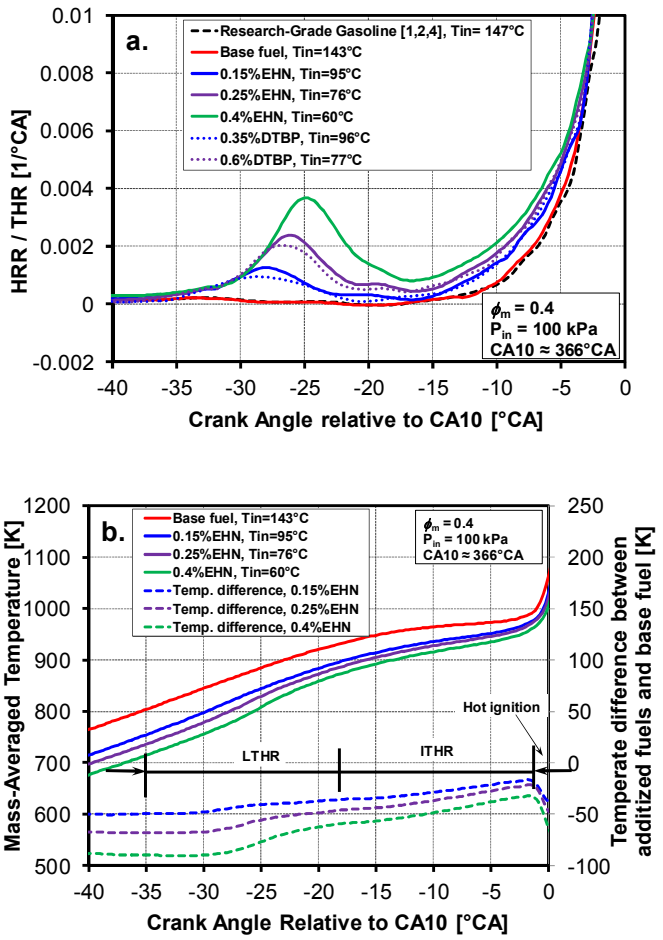

Figure 6. Effect of EHN and DTBP on HRR and temperature at low and intermediate temperature range: (a) HRR and (b) temperature profiles at P_{in} = 100 kPa, ϕ_m = 0.4, and CA10 ≈ 366°CA without EGR or CSPd. The HRR of a research-grade conventional gasoline [1, 2, 4] at P_{in} = 100 kPa is also plotted in Fig. 6a for comparison.

As shown in Fig. 6a, fuels with high additive concentrations tend to have a higher early HRR than the fuels with low or no additives. Thus, it is expected that the temperature should rise faster for additized fuels compared with base fuel. The mass-averaged temperature computed from the cylinder pressure trace for fuels with various EHN concentrations is shown in Fig. 6b. Also, at the bottom of Fig. 6b are plots of the temperature difference between the additized fuel and the base fuel, for a more clear comparison. Compared with the base fuel, the gas temperature is lower for the additized fuels before the point that any chemistry occurs (< 330°CA or -35°CA relative to CA10). This is due to the progressive reduction in required T_{in} with increased EHN concentration, as shown in the figure legend. The difference between the base fuel and the additized fuels remains nearly constant prior to the onset of LTHR since the γ's are similar. As the charge is compressed further, LTHR occurs (from about -35 to-18°CA relative to CA10), and fuels containing more EHN show a greater temperature rise due to their stronger LTHR (see Figs. 6a and 6b). As a result, the temperature difference between the base fuel and additized fuels is reduced by an amount proportional to the EHN concentration. The reduction of the temperature differences continues through the ITHR period (from about -18 to -2°CA relative to CA10) since the ITHR is also enhanced by an amount proportional to the EHN concentration (see Fig. 6a). Despite this substantial reduction in the temperature difference between the fuels, Fig. 6b shows that at the hot ignition point, the temperatures of the additized fuels are still lower than the temperature of the base fuel by an amount proportional to the EHN concentration, indicating differences in the hot-ignition chemistry. Fig. 6b also shows that the temperature difference starts becoming larger again after the hot ignition, which further indicates differences in the chemistry near the hot ignition point as a result of the EHN and the differences in the LTHR and ITHR chemistry.

Similar observations and conclusions are also found for boosted operation. Fig. 7a and 7b show the HRR and temperature profiles prior to hot ignition for the base fuel and two additized fuels at P_{in} = 130 kPa, ϕ_m = 0.4, CSPd = 47.2%, and CA10 ≈ 366.9°CA. For these data, the T_{in}'s are at much higher values compared with those in Fig. 6a and 6b for P_{in} = 100 kPa. These high T_{in}'s were required despite the enhancement of autoignition by the intake boost, because of the large amount of CSPd (47.2%) used for these data. Similar to P_{in} = 100 kPa, the LTHR and ITHR are enhanced for additized fuels as shown in Fig. 7a. However, the increase in LTHR is much smaller than that observed for P_{in} = 100 kPa primarily because the high T_{in} used for the P_{in} = 130 kPa data mitigates the low-temperature chemistry (or alternatively, the lower T_{in} used for P_{in} = 100 kPa acts to increase the low-temperature chemistry). Corresponding to this low amount of LTHR, the charge temperature increases slightly during the LTHR period, as shown in Fig. 7b. Similarly, the enhancement of ITHR is relatively small for these higher T_{in} data, and somewhat surprisingly, the ITHRs for 0.4%EHN and 0.25%EHN appear to be quite similar (Fig. 7a). Despite the reduced enhancement of the LTHR and ITHR due to the relatively high T_{in}, Fig. 7b shows that they reduce the temperature difference between the additized fuels and base fuel with the same overall trend as observed for P_{in} = 100 kPa in Fig. 6b. Finally, it should be noted that in addition to the higher T_{in}, it is possible that the large amount of CSPd used for the boosted data reduces the effectiveness of the additives.

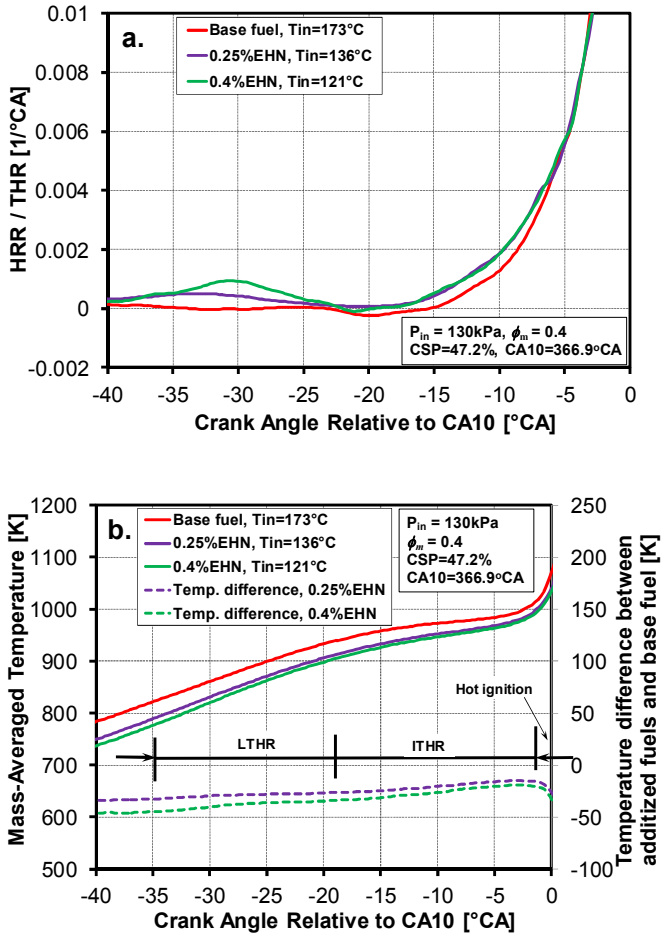

Figure 7. Effect of EHN and DTBP on HRR and temperature at low and intermediate temperature range: (a) HRR and (b) temperature profiles at P_{in} = 130 kPa, ϕ_m = 0.4, CSPd = 47.2%, and CA10 ≈ 366.9°CA.

In a summary, EHN and DTBP are shown to enhance the LTHR and ITHR, reduce the required T_{in}'s, and increase the autoignition reactivity. The following section investigates how the additives extend the high-load limits at various P_{in}'s considering their effectiveness in enhancing the HCCI reactivity.

High-load Limits

One of the goals of the current work is to determine the high-load limits as P_{in} varies from 100 kPa to 180 kPa and fuel reactivity changes with the amount of EHN and DTBP addition. For each P_{in} and fuel type, the fueling was increased from a moderate value up to the highest load possible. Increasing the fueling at a fixed P_{in} increases the PRR, eventually causing the engine to knock. In order to slow the HRR and reduce the PRR to prevent knock, the combustion phasing was retarded by adding EGR. On the other hand, combustion retard is eventually limited by poor combustion stability as manifested by excessive cycle-to-cycle variation in the $IMEP_g$. This occurs because the rate of charge cooling due to expansion increases with combustion retard. This cooling slows the early autoignition reactions generated by the low- and intermediate-temperature chemistry, thus reducing the rate of temperature rise toward the hot ignition point. As a result, the onset of hot ignition becomes more sensitive to small variations in T_{in} and wall temperature causing cycle-to-cycle variation in CA50 and $IMEP_g$ [36, 37]. Eventually, a point is reached as fueling is increased, where a further increase in load will cause the engine to knock, but CA50 can't be further retarded to prevent knock because the combustion becomes unstable and extremely difficult to control. This point is the knock/stability limit. For such a limit, the maximum fueling rate is determined by the amount of combustion-phasing retard that can be applied with acceptable combustion stability.

Previous studies [3, 4] have shown that the combustion phasing can be further retarded with good stability if the HRR before the hot ignition point (*i.e.* the ITHR) can be enhanced. For these conditions, the enhanced early HRR compensates for the greater expansion cooling rate, resulting in a higher temperature rise rate (TRR) for retarded combustion phasing. This behavior has been achieved by either increasing the boost level [4] or using a low-octane (high reactivity) fuel [3], both of which can enhance the ITHR. A combination of intake-temperature reduction and cooled EGR addition can be used to achieve the necessary combustion-phasing retard for such conditions. To prevent fuel from condensing in the intake system, the lowest allowable T_{in} was kept at 60°C for the current study. Therefore, adjusting the EGR becomes the only option for combustion-phasing control for conditions with higher boost or more highly reactive fuels that would otherwise require a T_{in} < 60°C. However, the addition of EGR reduces the intake O_2 concentration, and this can limit the load for conditions that are not knock/stability limited. As fueling is increased for these conditions, eventually, the conventional □ increases to near the stoichiometric point, for which exhaust O_2 levels are near zero. As this stoichiometric point is approached, combustion efficiency begins to drop causing a reduction in thermal efficiency and $IMEP_g$. This point is the oxygen/stoichiometric limit. For such a limit, the maximum fueling rate is determined by the intake O_2 concentration, which varies with the amount of EGR required.

For the various boost levels and fuel mixtures investigated, the maximum load may be limited by either the knock/stability limit or the oxygen/stoichiometric limit. To investigate this behavior, and further understand the effect of EHN and DTBP on high-load limits, the remainder of this section discusses the high-load limits for CCG-E10 and mixtures of CCG-E10 with various amounts of EHN and DTBP over a range of intake pressures. The ringing intensity was kept to 5 MW/m^2 to prevent knock, except for the cases indicated.

Figure 8 shows the $IMEP_g$ and exhaust O_2 concentrations as a function of ϕ_m at different P_{in}'s for fully premixed CCG-E10 and CCG-E10 with 0.4%EHN. Both kinds of high-load limits were observed in this set of experiments. The knock/stability limits occur at the conditions with low boost and low fuel reactivity, and oxygen/stoichiometric limits occur at higher boost levels with higher-reactivity fuels. More specifically, for unadditized CCG-E10, the maximum loads at all P_{in}'s are limited by stability as show in open red symbols in Fig. 8. It is interesting to see that the maximum loads for all P_{in}'s for this fuel occur at about the same ϕ_m = 0.47. No EGR was used for P_{in} = 100 kPa and 130 kPa since the reactivity of CCG-E10 is low and higher T_{in}'s are required as shown in Fig. 8a. After the boost level increases to 160 and 180 kPa, T_{in} was kept at 60°C and EGR

was added to retard CA50 to prevent knock. But the amount of EGR required is low, and plenty of oxygen is available before the knock/stability limit occurs.

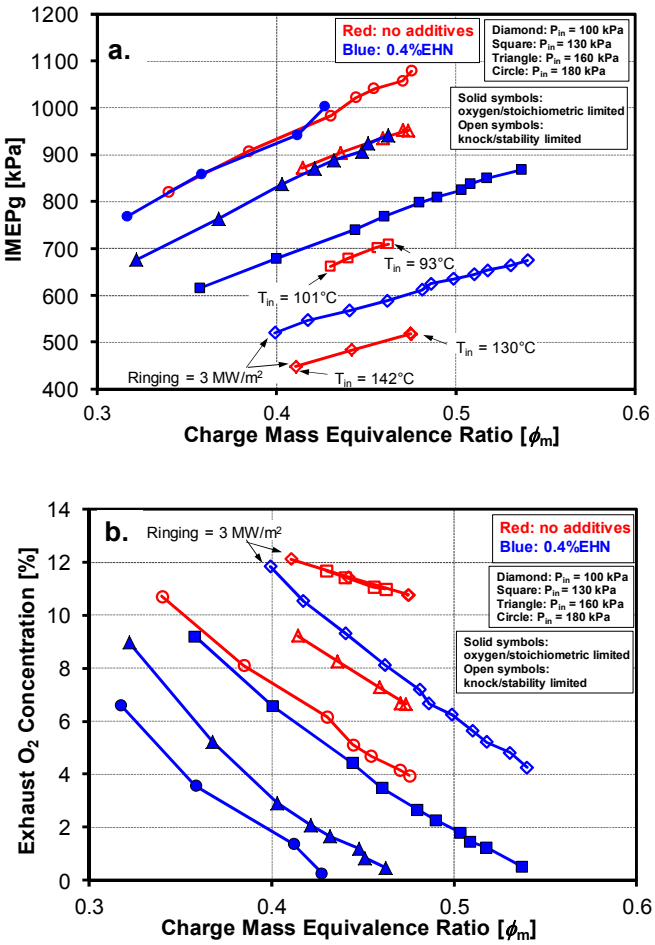

Figure 8. (a) $IMEP_g$ and (b) exhaust oxygen concentrations vs. ϕ_m at various P_{in}'s for fully premixed CCG-E10 and CCG-E10 with 0.4%EHN. For both plots, the symbols represent: (Red) CCG-E10, (Blue) CCG-E10 with 0.4%EHN; (Open) maximum load limited by stability, i.e., knock/stability limit, (Solid) maximum load limited by a lack of oxygen, i.e., oxygen/stoichiometric limit; (Diamond) P_{in} = 100 kPa, (Square) P_{in} = 130 kPa, (Triangle) P_{in} = 160 kPa, (Circle) P_{in} = 180 kPa. T_{in} = 60°C for all the operating conditions except for base fuel at P_{in} = 100 kPa with 130°C ≤ T_{in} ≤ 142°C and P_{in} = 130 kPa with 93°C ≤ T_{in} ≤ 101°C as noted in Fig. 8a. Higher T_{in}'s are required for lower ϕ_m's for the base fuel at P_{in} = 100 kPa and P_{in} = 130 kPa due to the low auto-ignition reactivity. Ringing intensity = 5 MW/m^2 except for both fuels at P_{in} = 100 kPa with ringing intensity = 3 MW/m^2.

However, for CCG-E10 with 0.4%EHN, the maximum load is limited by the knock/stability limit only at P_{in} = 100 kPa. For all the boost levels from 130 to 180 kPa, the maximum loads are limited by lack of oxygen as shown indicated by the solid blue symbols in Fig. 8. All the results for CCG-E10 with 0.4%EHN are conducted at T_{in} = 60°C with EGR due to its high reactivity. For P_{in} = 100 kPa, CCG-E10 with 0.4%EHN shows a higher $IMEP_g$ than unadditized CCG-E10 at a given ϕ_m. This is due to a higher charge density for CCG-E10 with 0.4%EHN because of the lower T_{in} = 60°C compared with that of unadditized CCG-E10 at T_{in} = 130°C. The same observation is found for P_{in} = 130 kPa, although the difference is now smaller due to a small discrepancy in T_{in}. If T_{in}'s are the same, the difference in $IMEP_g$ between base fuel and additized fuel is negligible at a given ϕ_m as shown for the P_{in} = 160 and 180 kPa in Fig. 8a. Fig. 8a also shows that due to the enhanced HCCI reactivity (*i.e.* strong ITHR), CCG-E10 with 0.4%EHN can achieve a much higher ϕ_m (≈ 0.54) at P_{in} = 100 and 130 kPa compared with a maximum ϕ_m ≈ 0.47 for unadditized CCG-E10. This effect combined with the lower T_{in} result in an increase of 30% and 22% in maximum load for the additized fuel at P_{in} = 100 and 130 kPa respectively. These results are inspiring considering the small amount of additive used. However, for a boost level of 160 kPa, the high reactivity of CCG-E10 with 0.4%EHN has a slight negative effect on the maximum achievable load, reducing it by about 1% compared to the base fuel. This effect becomes larger as P_{in} is further increased to 180 kPa, where the maximum load is 7% lower for the CCG-E10 with 0.4%EHN. As can be seen, the lower maximum loads for the additized fuel at P_{in} = 160 and 180 kPa result from a lower maximum ϕ_m's. Figure 8b shows that this is due to the high levels of EGR required to control CA50, which reduce the amount of oxygen available for combustion, so the maximum ϕ_m's for P_{in} = 160 and 180 kPa are at the oxygen/stoichiometric limit.

It appears that there is a trade-off between improved stability and reduced O_2 when using these additives. To further illustrate this point, Fig. 9 shows the maximum $IMEP_g$ and corresponding exhaust O_2 concentration as a function of P_{in}. As shown in Fig. 9a, the maximum $IMEP_g$ increases with P_{in} for all the fuels. The trend keeps a constant slope if the high-load limit remains the same type such as the case for CCG-E10 without any additives. However, the slope changes if there is a transition from a knock/stability limit to an oxygen/stoichiometric limit like the cases for CCG-E10 with additive. The transition occurs at a lower P_{in} for fuels with higher additive concentration as shown in Fig. 9. For example, for CCG-E10 with 0.35%DTBP, which is similar with CCG-E10 with 0.15%EHN as discussed above, the transition occurs at 160 kPa, where the HCCI combustion reaches both knock/stability and oxygen/stoichiometric limits as shown in Fig. 9b. When the EHN percentage increases to 0.25%, the transition occurs at 130 kPa, and again, both knock/stability and oxygen/stoichiometric limits are reached at the same $IMEP_g$. For an EHN level of 0.4%, the transition occurs somewhere between P_{in} = 100 and 130 kPa, since the maximum load is already at the oxygen limit for P_{in} = 130 kPa.

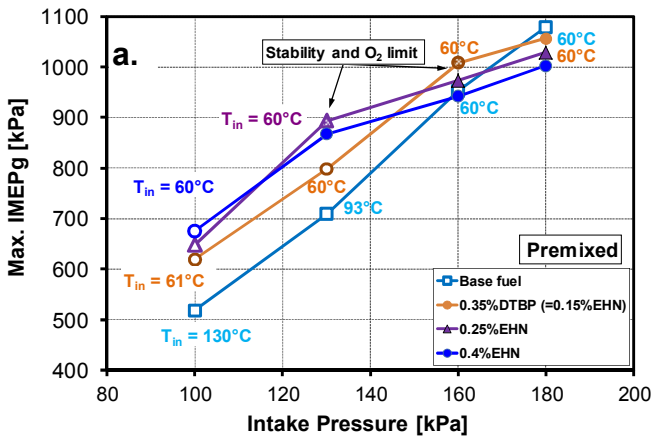

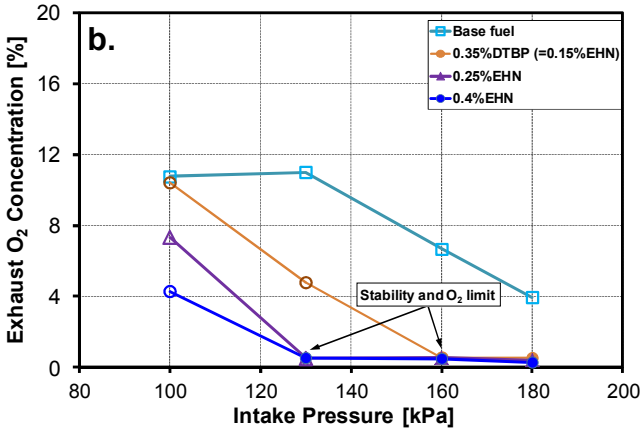

Figure 9. (a) Maximum $IMEP_g$ and (b) exhaust oxygen concentrations vs. P_{in}'s for different level of additives. Open symbols represent the knock/stability limit and solid symbols represent the oxygen/stoichiometric limit. Half-filled symbols represent that the point is achieved at both knock/stability and oxygen/stoichiometric limits. Ringing intensity = 5 MW/m^2 except for P_{in} = 100 kPa with ringing intensity = 3 MW/m^2.

The additive concentration can affect the maximum achievable load for a given P_{in} as shown in Fig. 9a. More specifically, Fig. 10 shows the maximum $IMEP_g$ as a function of additive concentration at each P_{in}. As the plot depicts, the maximum load can be increased by increasing the amount of additive if the reactivity of the fuel is low and it shows a knock/stability limit for a given P_{in}. However, once the fuel reaches the oxygen/stoichiometric limit, further increases in additive concentration will reduce the maximum $IMEP_g$. Thus, there exists an optimal value of additive concentration for each P_{in}, which allows the fuel to reach the highest load at that boost pressure. Consequently, these highest-load points must occur at both knock/stability and oxygen/stoichiometric limits.

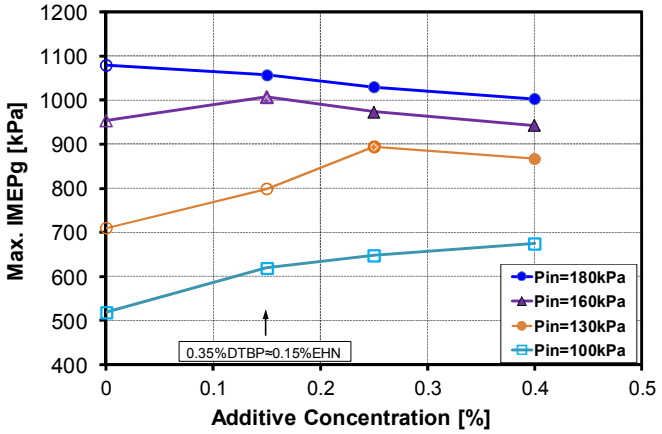

Figure 10. Maximum $IMEP_g$ varies as a function of additive concentration. The data reported at 0.35%DTBP is assumed to be the same at 0.15%EHN and thus can be comparable with fuels at different levels of EHN. Ringing intensity = 5 MW/m^2 except for P_{in} = 100 kPa with ringing intensity = 3MW/m^2.

Φ-Sensitivity and Partial Fuel Stratification

Previous studies [1, 6, 29, 35] have shown that ϕ-sensitivity is a key parameter in applying PFS because it allows the autoignition to occur sequentially down the equivalence ratio gradient, which reduces the HRR. Similar to the research-grade conventional gasoline with no ethanol used in previous studies [1-4], the low-reactivity base fuel, CCG-E10, shows essentially no ϕ-sensitivity at naturally aspirated conditions as shown in Fig. 11. However, strong ϕ-sensitivity can be achieved with sufficient boost since the increasing P_{in} enhances the fuel reactivity (ITHR). The increase in ϕ-sensitivity with boost for CCG-E10 is quite similar to that of the conventional gasoline, since the two fuels have nearly the same ϕ-sensitivity at P_{in} = 200 kPa as well as P_{in} = 100 kPa, as can be seen in Fig. 11. Fuel ϕ-sensitivity has been found to correlate with ITHR as discussed in Ref. 29. More specifically, fuels with strong ITHR show a strong ϕ-sensitivity. As shown in Fig. 6a, it is expected that additized fuels should have stronger ϕ-sensitivity than the base fuel because the additives enhance the ITHR.

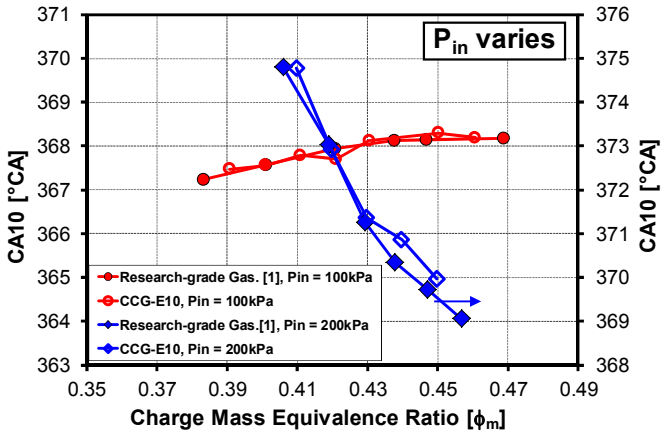

Figure 11. ϕ-sensitivity of CCG-E10 and a research-grade gasoline (from Ref. [1]) at P_{in} = 100 and 200 kPa.

Figure 12 shows the ϕ-sensitivities of the base fuel and additized fuels at P_{in} = 100 and 130 kPa. At naturally aspirated conditions, the ϕ-sensitivity is significantly enhanced by adding 0.4%EHN as shown in the figure. For comparison purposes, the ϕ-sensitivity of PRF73 (73% *iso*-octane and 27% *n*-heptane by volume) at P_{in} = 100 kPa (from Ref. 29) is also plotted in Fig. 12. As can be seen, CCG-E10 with 0.4%EHN shows a slightly stronger ϕ-sensitivity than PRF73. Considering the low concentration of EHN, ignition-improving additives appear to be a very effective method for enhancing the ϕ-sensitivity, and therefore, they have a strong potential for allowing the beneficial application of PFS. The same conclusion can be drawn for boosted P_{in}. At P_{in} = 130 kPa, CCG-E10 shows slightly stronger ϕ-sensitivity than at P_{in} = 100 kPa. But this moderate enhancement in ϕ-sensitivity, due only to the increase of P_{in}, is not sufficient for PFS to work well. However, by adding 0.35%DTBP, the fuel shows strong ϕ-sensitivity at P_{in} = 130 kPa. In fact, it is the strongest ϕ-sensitivity of all the fuels and conditions tested.

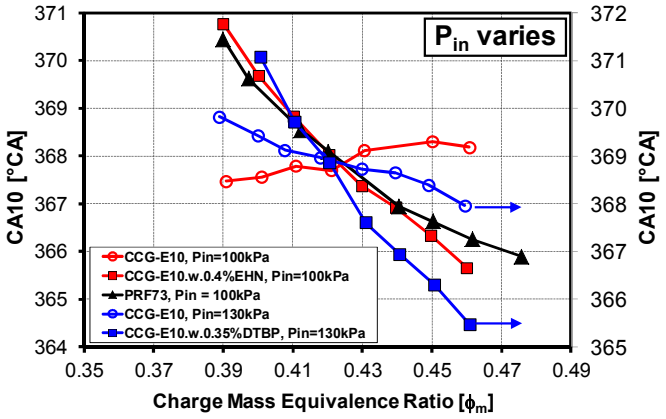

Figure 12. ϕ-sensitivity of CCG-E10 and CCG-E10 with additives at P_{in} = 100 (0.4%EHN) and 130 kPa (0.35%DTBP). For comparison purposes, the ϕ-sensitivity of PRF73 at P_{in} = 100 kPa from Ref. 29 is also plotted.

Given this strong enhancement in ϕ-sensitivity by adding EHN and DTBP, it is expected that PFS will work well for additized fuels to improve the thermal efficiency of the engine. Figure 13a compares the gross indicated thermal efficiency for fully premixed (PM) and PFS conditions for fuels with different EHN concentrations at two P_{in}'s. The PFS parameters are given in the figure caption, and it should be noted that T_{in} = 60°C and the Ringing Intensity = 5 MW/m^2 for all data presented.

For the fuel with 0.4%EHN at P_{in} = 100kPa, applying PFS increases the thermal efficiency over the entire load range compared to fully premixed condition. The maximum increase is around 0.4 - 0.5 thermal-efficiency percentage-units at low-to-middle part of the IMEP$_g$ range. For the higher part of the load range, PFS provides less improvement. The increase in thermal efficiency with PFS is largely the result of it allowing the combustion phasing to be more advanced while still maintain a ringing intensity of 5 MW/m^2. This improvement in thermal efficiency occurs despite the slightly lower combustion efficiency with PFS shown in Fig. 13c.

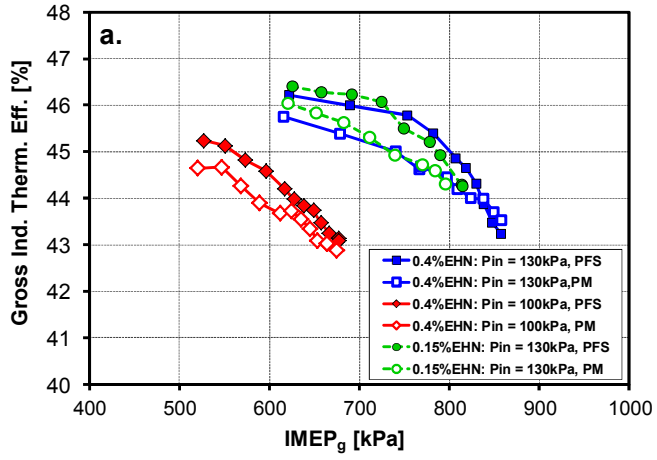

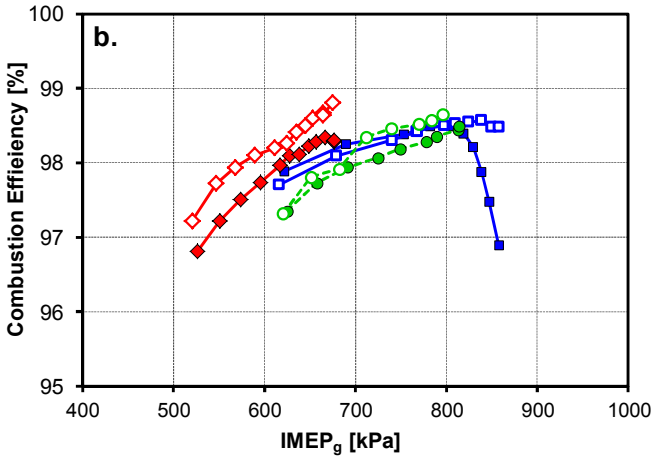

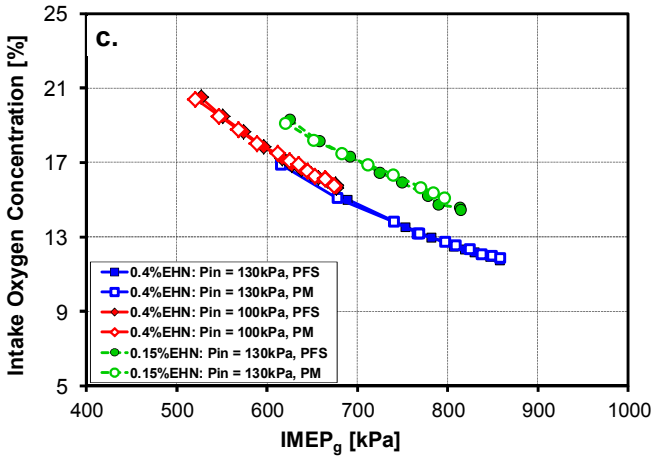

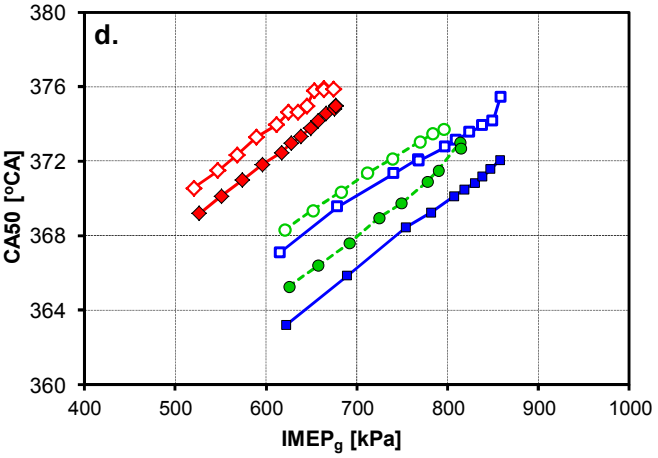

Figure 13. Comparison of HCCI performance with partial fuel stratification (PFS) and fully premixed (PM) charge for CCG-E10 with various EHN concentrations at P_{in} = 100 and 130 kPa. The legend shown in Fig. 13a and 13c applies to all figures. For all data shown, T_{in} = 60°C, DI injection pressure (P_{inj}) = 135 bar, and the Ringing Intensity = 5 MW/m^2. 5% DI at SOI = 310°CA was used for CCG-E10 with 0.4%EHN at P_{in} = 100kPa, 10%DI at SOI = 310°CA for CCG-E10 with 0.4%EHN at P_{in} = 130kPa, and 10%DI at SOI = 300°CA for CCG-E10 with 0.15%EHN at P_{in} = 130kPa except for the highest load with 5%DI at SOI = 310°CA.

Increasing P_{in} to 130 kPa significantly increases the thermal efficiency compared to P_{in} = 100 kPa for both PM and PFS operation as can be seen in Fig. 13a. This is mainly because CA50 can be more advanced for the same ringing intensity with a higher P_{in} (see Fig. 13d). For the fuel with 0.4%EHN at P_{in} = 130kPa, applying PFS only increases the thermal efficiency over the low-to-middle part of the load range compared to PM operation, similar to P_{in} = 100 kPa. However, unlike P_{in} = 100 kPa, the thermal efficiency for PFS drops dramatically at high loads, and even falls slightly below the PM values near the high-load limit (Fig. 13a). This is because the high-load limit for this fuel at P_{in} = 130kPa is an oxygen limit, and with PFS, there is a rapid decrease of combustion efficiency as this limit is approached (Fig. 13b). The reason this occurs is that the fuel stratification with PFS produces regions that are locally richer, and as the fueling is increased to the limit, these regions have insufficient oxygen, resulting in incomplete combustion even though there is still oxygen available in other parts of the charge. Thus, even though the overall intake oxygen concentrations are the same for PM and PFS, as shown in Fig. 13c, the combustion efficiency of PFS falls much more quickly near the oxygen limit, which reduces the thermal efficiency of PFS compared to PM despite CA50 still being more advanced, as shown in Fig. 13d.

To overcome this disadvantage, a fuel with 0.15%EHN was tested at P_{in} = 130kPa and the results are also shown in Fig. 13. Due to the lower reactivity of the fuel with 0.15%EHN compared to fuel with 0.4%EHN, less EGR is required, and more oxygen is available as shown in Fig. 13c. Under such circumstances, PFS increases the thermal efficiency over the entire $IMEP_g$ range investigated with a trend similar to that found for the fuel with 0.4%EHN at P_{in} = 100kPa. It should be noted that although adjusting the additive concentration can avoid the oxygen limit and allow PFS work near the high-load limit, it also turns the oxygen/stoichiometric limit into a knock/stability limit, which reduces the maximum load, as shown in Fig. 13a. At P_{in} = 130kPa, PFS increase the thermal efficiency by 0.6 - 0.8 percentage-units in the low-to-middle part of the $IMEP_g$ range, which is 0.2 - 0.3 percentage-units more than the increase at P_{in} = 100kPa (Fig. 13a). The main reason is thought to be that a 10% DI fuel fraction was used at P_{in} = 130kPa and compared to a 5% DI fraction at P_{in} = 100kPa. A greater DI fraction tends to increase the fuel stratification allowing the combustion phasing to be more advanced, as shown in Fig. 13d. Figure 13a also shows that the fuel with 0.15%EHN gives a slightly higher thermal efficiency at low loads compared to the fuel 0.4%EHN, for both PM and PFS conditions, despite its slightly lower combustion efficiency (Fig. 13b). This is largely because less EGR is required for the fuel with 0.15%EHN, as shown in Fig. 13c.

In the current study, PFS was found to marginally increase the high-load limit. Except for the fuel with 0.4%EHN at P_{in} = 130kPa, which is limited by lack of oxygen, PFS did not show an increase in the stability of HCCI combustion near the knock/stability limit. For the fuel with 0.4%EHN at P_{in} = 100kPa and the fuel with 0.15%EHN at P_{in} = 130kPa, the maximum load is virtually the same for either PFS or PM fueling, even though PFS allows CA50 to be more advanced at knock/stability limit. Various combinations of DI fraction and DI timing were attempted for the fuel with 0.15%EHN at P_{in} = 130kPa, but the increase in high-load limit over PM operation is very modest as shown in Fig. 13a.

In summary, PFS is shown to effectively increase the thermal efficiency for fuels with additives. By applying different additive concentrations and adjusting the DI timing and DI fraction, PFS has strong potential to further increase the efficiency at various loads and boosted levels.

NOx EMISSIONS

As discussed in the introduction, increased NOx emissions are one of the concerns when using EHN as an ignition-improving additive. Figure 14 shows the NOx emissions as a function of ϕ_m at various P_{in}'s for both base fuel alone and with 0.4%EHN. For the base fuel with no additives, NOx emissions are found to be much higher at naturally aspirated conditions than at boosted conditions, as shown in Fig. 14 and in previous study [4]. One of the major reasons is the high peak charge temperature (T_{peak}), which results from the high required T_{in}. Lower T_{in} is required at boosted conditions, and thermal NOx is reduced significantly as T_{peak} decreases. As shown in Fig. 15, T_{peak} is about 70 - 90 K higher at P_{in} = 100 kPa than that at P_{in} = 180 kPa for CCG-E10 at each given ϕ_m.

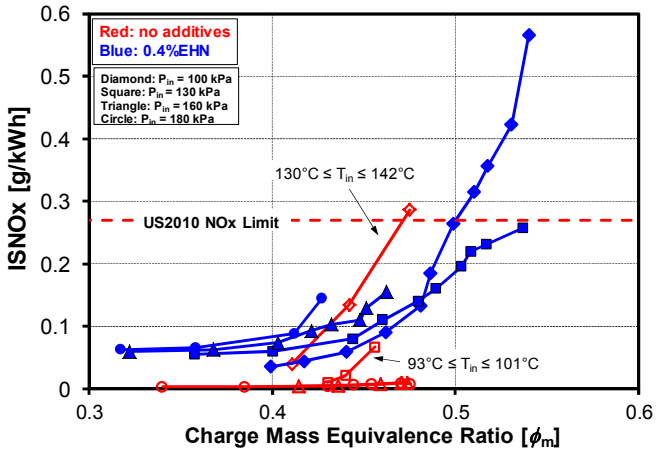

Figure 14. NOx emissions vs. ϕ_m at varied P_{in}'s for fully premixed CCG-E10 and CCG-E10 with 0.4%EHN. The open red symbols represent NOx emission from CCG-E10 and the solid blue symbols represent CCG-E10 with 0.4%EHN. T_{in} = 60°C for all the operating conditions except for the base fuel (CCG-E10) at P_{in} = 100 kPa with T_{in} = 130°C and P_{in} = 130 kPa with T_{in} = 93°C for the maximum loads. Ringing intensity = 5 MW/m^2 except for both fuels at P_{in} = 100 kPa with ringing intensity = 3 MW/m^2.

Except for P_{in} = 100 kPa, the additized fuel shows consistently higher NOx emissions compared with the base fuel (see Fig. 14). At P_{in} = 100 kPa, thermal NOx is considered to be the major source contributing to the higher NOx emissions for base fuel. For example, T_{peak} of unadditized CCG-E10 is 70 - 80 K higher than that of CCG-E10 with 0.4%EHN for a given ϕ_m (see Fig. 15), due to the higher required T_{in}, as noted on Fig. 14 and in the figure caption. It can also be seen that, for CCG-E10 with 0.4% EHN, ϕ_m could be increased well above the maximum ϕ_m for unadditized CCG-E10, and with this higher fueling, the NOx emissions increase above those of unadditized CCG-E10. However, since T_{peak} for these higher-ϕ_m additized-fuel data points is ≤ T_{peak} for the unadditized CCG-E10, except for the highest ϕ_m point, the EHN must be contributing to the NOx increase above that of the base fuel.

For P_{in} = 180 kPa, the effect of the EHN is even more clearly evident. At this boosted P_{in}, T_{in} = 60°C for both the base and additized fuels, and T_{peak} at a given ϕ_m is also nearly identical, as shown in Fig. 15. Thus, the higher NOx emissions for the fuel containing EHN must be related to the nitrate group in EHN. Similarly, the EHN must be enhancing the NOx emissions for the other intake pressures shown in Fig. 14.

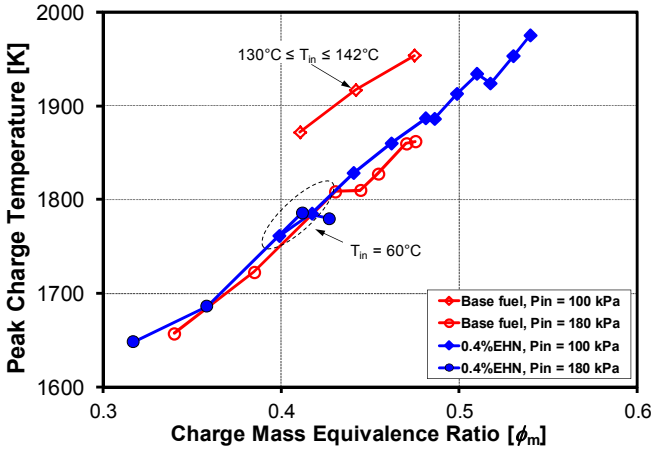

Figure 15. Peak charge temperature (mass-averaged), T_{peak} vs. ϕ_m for P_{in} = 100 and 180 kPa. T_{in} = 60°C for all the operating conditions except for the base fuel (CCG-E10) at P_{in} = 100 kPa where 130°C ≤ T_{in} ≤ 142°C for 0.475 ≥ ϕ_m ≥ 0.415, respectively. Ringing intensity = 5 MW/m^2 except for P_{in} = 100 kPa with ringing intensity = 3 MW/m^2.

More specifically, the NOx emissions increase with increasing EHN concentration (see Fig. 16a). On the other hand, with the DTBP additive, a slight yet notable decrease of NOx emissions is found. As shown in Fig. 16b, increasing DTBP reduces T_{in} and T_{peak}, which slightly reduce the thermal NOx. Increasing EHN also reduces T_{in} and T_{peak}, but the effect on the reduction of thermal NOx is smaller than the NOx produced from the nitrate group in EHN. Also plotted in Fig. 16a are the NOx emissions that would be produced assuming all of the nitrate groups in the EHN are converted to NOx. Comparison of the two curves indicates that the actual conversion rate of the nitrate groups in EHN to NOx is about 30%, which is consistent with the results reported by Ickes et al. [26]. NOx emissions at boosted conditions are shown in Fig. 17. Similar to P_{in} = 100 kPa, NOx is reduced slightly for increasing DTBP at P_{in} = 130kPa because of the decrease of T_{in} (see Fig. 17a). If T_{in} stays constant, increasing DTBP has almost no effect on NOx emissions as shown in Fig. 17b for P_{in} = 180 kPa. On the other hand, NOx emissions increase with increasing EHN concentration at both P_{in} = 130 and 180 kPa, despite the decrease of T_{in} at P_{in} = 130 kPa.

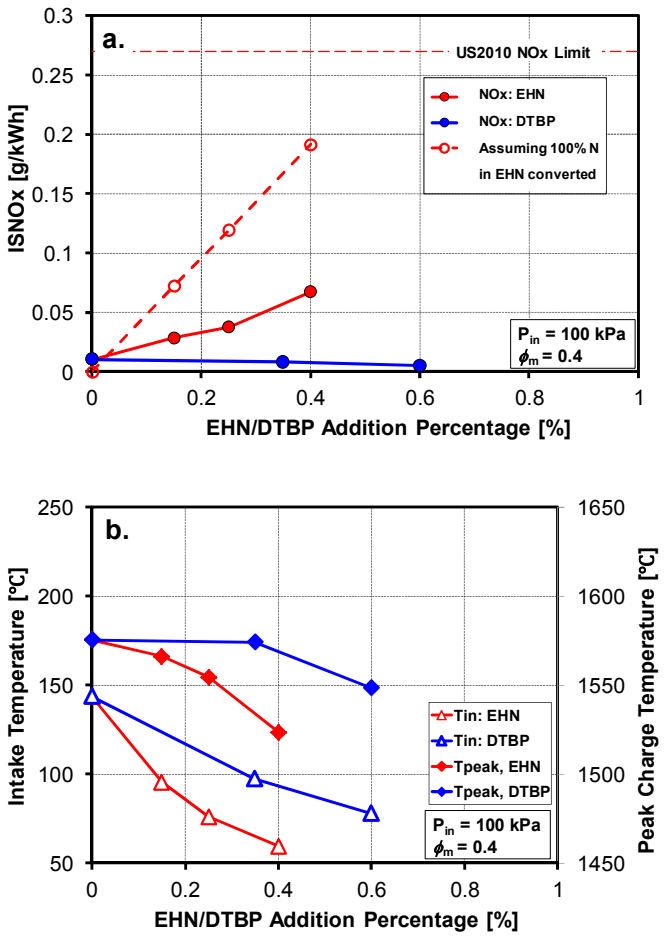

Figure 16. (a) NOx emission and (b) intake temperature and peak charge temperature (mass-averaged) vs. additive concentration at P_{in} = 100 kPa and ϕ_m = 0.4.

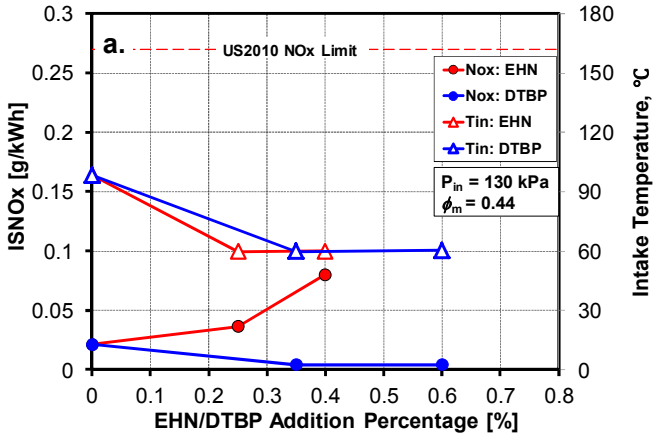

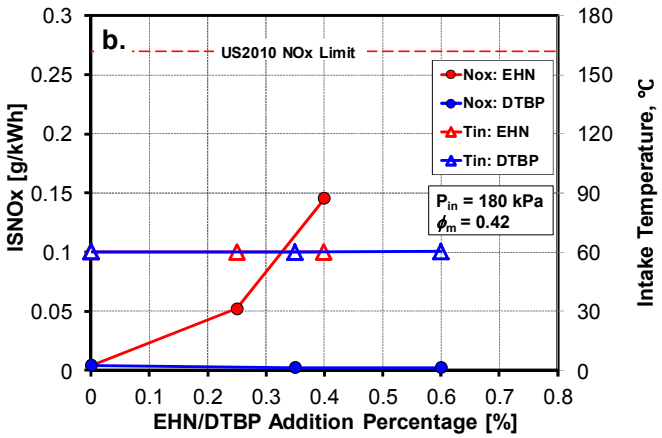

Figure 17. NOx emissions and intake temperature vs. additive concentration at (a) P_{in} = 130 kPa and (b) P_{in} = 180 kPa.

In summary, DTBP has almost no effect on NOx emissions but nearly 30% of the nitrate groups in EHN convert to NOx and increase the NOx emissions. However, the NOx emissions are still acceptable and below the US-2010 standard at boosted conditions.

Summary/Conclusions

The effect of conventional ignition improvers 2-ethylhexyl nitrate (EHN) and di-tert-butyl peroxide (DTBP) on the autoignition reactivity of gasoline in an HCCI engine has been studied in the present work over a range of intake pressures (P_{in} = 100~180kPa) and fueling rates. The autoignition reactivity, high-load limits, NOx emissions, and application of partial fuel stratification have been investigated. The following conclusions can be drawn.

1. Both EHN and DTBP are effective for enhancing the HCCI autoignition reactivity of regular gasoline. T_{in} can be reduced significantly with a very small amount of additives (<0.6%) at naturally aspirated conditions. More than double the amount of DTBP is required to get the same reactivity as EHN.
2. The LTHR and ITHR of the gasoline fuel are progressively enhanced with increasing EHN and DTBP concentrations when combined with progressively reduced Tin to maintain combustion phasing. The enhancement is significant even at naturally aspirated conditions (P_{in} = 100kPa). The increased ITHR counteracts the effects of expansion cooling, allowing significantly greater combustion phasing retard with good stability. With greater CA50 retard, the fueling rate (ϕ_m) can be increased to obtain higher loads without knock.
3. The reduction in required Tin with ignition-improving additives significantly increases the charge density with a commensurate increase in $IMEP_g$. This effect, combined with the greater allowable CA50 retard, allows the high-load limit to be increased substantially at naturally aspirated and low-boost conditions, 30% at P_{in} = 100 kPa and 22% at P_{in} = 130 kPa.
4. Increasing the intake-boost pressure also enhances the autoignition, and the additized gasoline can become very reactive as boost level is increased, requiring a large amount of EGR to prevent overly advanced autoignition. These high EGR levels reduce the amount of oxygen in the charge, and the maximum load becomes limited by oxygen availability before it reaches the knock/stability limit.
5. There is a trade-off between the advantages of enhanced fuel reactivity with additive addition and the reduction in available oxygen due to required EGR addition. An optimal amount of EHN/DTBP can be chosen to maximize the load for a given P_{in}, which allows the fuel to achieve the knock/stability and oxygen-availability limits at the same time.
6. Adding EHN or DTBP increases the ϕ-sensitivity of the autoignition reactions, and this enhancement can be varied by the adjusting the additive concentration. With this enhanced ϕ-sensitivity, PFS becomes effective for reducing the HRR for regular gasoline even at naturally aspirated and low-boost conditions.
7. Applying PFS reduces the HRR and the associated maximum PRR, thus allowing CA50 to be advanced to increase the thermal efficiency while maintaining an acceptable ringing intensity. By optimizing additive concentrations and the DI timing, PFS has a strong potential to further increase engine efficiency at various loads and boost levels.
8. EHN produces a small increase in the NOx emissions for HCCI combustion approximately proportional to the additive concentration. About 30% of the nitrate groups in the EHN are converted to NOx. Although the total amount of NOx is still below the US2010 standard for most conditions, the effect of EHN on NOx emissions is not negligible. In contrast, DTBP has no effect on NOx emissions.

In summary this work indicates that conventional cetane improvers provide a practical method for enhancing the autoignition reactivity of regular gasoline, which can be used to improve the performance of HCCI combustion.

References

1. Dec, J, Yang, Y., and Dronniou, N., “Boosted HCCI – controlling pressure-rise rate for performance improvements using partial fuel stratification with conventional gasoline,” *SAE Int. J. Engines* 4(1): 1169-1189, 2011, doi: 10.4271/2011-01-0897.
2. Dec, J., Yang, Y., and Dronniou, N., "Improving Efficiency and Using E10 for Higher Loads in Boosted HCCI Engines," *SAE Int. J. Engines* 5(3):1009-1032, 2012, doi:10.4271/2012-01-1107.
3. Yang, Y., Dec, J., Dronniou, N., and Cannella, W., "Boosted HCCI Combustion Using Low-Octane Gasoline with Fully Premixed and Partially Stratified Charges," *SAE Int. J. Engines* 5(3):1075-1088, 2012, doi:10.4271/2012-01-1120.
4. Dec, J., and Yang, Y., “Boosted HCCI for high power without engine knock and with ultra-low NOx emissions – using conventional gasoline,” *SAE Int. J. Engines* 3(1): 750-767, 2010, doi: 10.4271/2010-01-1086.
5. Sjöberg, M. and Dec, J., "Combined Effects of Fuel-Type and Engine Speed on Intake Temperature Requirements and Completeness of Bulk-Gas Reactions for HCCI Combustion," SAE Technical Paper 2003-01-3173, 2003, doi:10.4271/2003-01-3173.

6. Dec, J. and Sjöberg, M., "Isolating the Effects of Fuel Chemistry on Combustion Phasing in an HCCI Engine and the Potential of Fuel Stratification for Ignition Control," SAE Technical Paper 2004-01-0557, 2004, doi:10.4271/2004-01-0557.
7. Christensen, M., Johansson, B., Amnéus, P., and Mauss, F., "Supercharged Homogeneous Charge Compression Ignition," SAE Technical Paper 980787, 1998, doi:10.4271/980787.
8. Christensen, M. and Johansson, B., "Supercharged Homogeneous Charge Compression Ignition (HCCI) with Exhaust Gas Recirculation and Pilot Fuel," SAE Technical Paper 2000-01-1835, 2000, doi:10.4271/2000-01-1835.
9. Bessonette, P., Schleyer, C., Duffy, K., Hardy, W. et al., "Effects of Fuel Property Changes on Heavy-Duty HCCI Combustion," SAE Technical Paper 2007-01-0191, 2007, doi:10.4271/2007-01-0191.
10. Krisman, A., Hawkes, E.R., Kook, S., Sjöberg, M., Dec, J.E., "On the potential of ethanol fuel stratification to extend the high load limit in stratified-charge compression-ignition engines," *Fuel* 99: 45-54, 2012, doi: 10.1016/j.fuel.2012.04.001.
11. Han, X., Zheng, M., Wang, J., "Fuel suitability for low temperature combustion in compression ignition engines," *Fuel* 109: 336-349, 2013, doi: 10.1016/j.fuel.2013.01.049.
12. Yu, C., Wang, J., Wang, Z., Shuai, S., "Comparative study on Gasoline Homogeneous Charge Induced Ignition (HCII) by diesel and Gasoline/Diesel Blend Fuels (GDBF) combustion," *Fuel* 106: 470-477, 2013, doi: 10.1016/j.fuel.2012.10.068.
13. Starck, L., Lecointe, B., Forti, L., Jeuland, N., "Impact of fuel characteristics on HCCI combustion: Performances and emissions," *Fuel* 89 (10): 3069-3077, 2010, doi: 10.1016/j.fuel.2010.05.028.
14. Dec, J., "Advanced compression-ignition engines—understanding the in-cylinder processes," *Proc. Combust. Inst.* 32(2): 2727–2742, 2009, doi: 10.1016/j.proci.2008.08.008.
15. Machrafi, H., Cavadias, S., Gilbert, P., "An experimental and numerical analysis of the HCCI auto-ignition process of primary reference fuels, toluene reference fuels and diesel fuel in an engine, varying the engine parameters," *Fuel Processing Technology* 89(11): 1007-1016, 2008, doi: 10.1016/j.fuproc.2008.03.007.
16. Lu, X., Shen, Y., Zhang, Y., Zhou, X., Ji, L., Yang, Z., Huang, Z., "Controlled three-stage heat release of stratified charge compression ignition (SCCI) combustion with a two-stage primary reference fuel supply," *Fuel* 90(5): 2026-2038, 2011, doi: 10.1016/j.fuel.2011.01.026.
17. Guidance on Quantifying NOx Benefits for Cetane Improvement Programs for Use in SIPs and Transportation Conformity EPA420-B-04-005, June 2004.
18. Hanson, R., Kokjohn, S., Splitter, D., and Reitz, R., "Fuel Effects on Reactivity Controlled Compression Ignition (RCCI) Combustion at Low Load," *SAE Int. J. Engines* 4(1):394-411, 2011, doi:10.4271/2011-01-0361.
19. Kaddatz, J., Andrie, M., Reitz, R., and Kokjohn, S., "Light-Duty Reactivity Controlled Compression Ignition Combustion Using a Cetane Improver," SAE Technical Paper 2012-01-1110, 2012, doi:10.4271/2012-01-1110.
20. Hosseini, V., Neill, W.S., Guo, H., Chippior, W.L., Fairbridge, C., Mitchell, K., "Effects of different cetane number enhancement strategies on HCCI combustion and emissions," *Int. J. Engine Res.* 12: 89-108, 2011, doi: 10.1177/1468087410395873.
21. Eng, J., Leppard, W., and Sloane, T., "The Effect of Di-Tertiary Butyl Peroxide (DTBP) Addition to Gasoline on HCCI Combustion," SAE Technical Paper 2003-01-3170, 2003, doi:10.4271/2003-01-3170.
22. Mack, J., Dibble, R., Buchholz, B., and Flowers, D., "The Effect of the Di-Tertiary Butyl Peroxide (DTBP) additive on HCCI Combustion of Fuel Blends of Ethanol and Diethyl Ether," SAE Technical Paper 2005-01-2135, 2005, doi:10.4271/2005-01-2135.
23. Gong, X., Johnson, R., Miller, D., and Cernansky, N., "Effects of DTBP on the HCCI Combustion Characteristics of SI Primary Reference Fuels," SAE Technical Paper 2005-01-3740, 2005, doi:10.4271/2005-01-3740.
24. Gupta, A., Miller, D., and Cernansky, N., "A Detailed Kinetic Study on the Effect of DTBP on PRF Combustion in HCCI Engines," SAE Technical Paper 2007-01-2002, 2007, doi:10.4271/2007-01-2002.
25. Thompson, A., Lambert, S., and Mulqueen, S., "Prediction and Precision of Cetane Number Improver Response Equations," SAE Technical Paper 972901, 1997, doi:10.4271/972901.
26. Ickes, A.M., Bohac, S.V., Assanis, D.N., "Effect of 2-Ethylhexyl Nitrate cetane improver on NOx emissions from premixed low-temperature diesel combustion," *Energy and Fuels* 23 (10): 4943-4948, 2009, doi: 10.1021/ef900408e.
27. Bunting, B.G., Wildman, C.B., Szybist, J.P., Lewis, S., Storey, J., "Fuel chemistry and cetane effects on diesel homogeneous charge compression ignition performance, combustion, and emissions," *Journal of Engine Research* 8 (1): 15-27, 2007, doi: 10.1243/14680874JER01306.
28. Splitter, D., Reitz, R., and Hanson, R., "High Efficiency, Low Emissions RCCI Combustion by Use of a Fuel Additive," *SAE Int. J. Fuels Lubr*. 3(2):742-756, 2010, doi:10.4271/2010-01-2167.
29. Yang, Y., Dec, J., Dronniou, N., Sjöberg, M., "Tailoring HCCI heat release rates with partial fuel stratification: Comparison of two-stage and single-stage ignition fuels," *Proc. Combust. Inst.* 33 (2): 3047-3055, 2011, doi:10.1016/j.proci.2010.06.114.
30. Yang, Y., Dec, J., Dronniou, N., Sjöberg, M. et al., "Partial Fuel Stratification to Control HCCI Heat Release Rates: Fuel Composition and Other Factors Affecting Pre-Ignition Reactions of Two-Stage Ignition Fuels," *SAE Int. J. Engines* 4(1):1903-1920, 2011, doi:10.4271/2011-01-1359.
31. Dec, J. and Sjöberg, M., "A Parametric Study of HCCI Combustion - the Sources of Emissions at Low Loads and the Effects of GDI Fuel Injection," SAE Technical Paper 2003-01-0752, 2003, doi:10.4271/2003-01-0752.
32. Heywood, J.B., Internal Combustion Engine Fundamentals. New York: McGraw-Hill; 1988.
33. Eng, J., "Characterization of Pressure Waves in HCCI Combustion," SAE Technical Paper 2002-01-2859, 2002, doi:10.4271/2002-01-2859.
34. Sjoberg, M. and Dec, J., "Ethanol Autoignition Characteristics and HCCI Performance for Wide Ranges of Engine Speed, Load and Boost," *SAE Int. J. Engines* 3(1):84-106, 2010, doi:10.4271/2010-01-0338.
35. Sjöberg, M. and Dec, J., "Smoothing HCCI Heat-Release Rates Using Partial Fuel Stratification with Two-Stage Ignition Fuels," SAE Technical Paper 2006-01-0629, 2006, doi:10.4271/2006-01-0629.
36. Sjöberg, M., Dec, J., Babajimopoulos, A., and Assanis, D., "Comparing Enhanced Natural Thermal Stratification Against Retarded Combustion Phasing for Smoothing of

HCCI Heat-Release Rates," SAE Technical Paper 2004-01-2994, 2004, doi:10.4271/2004-01-2994.
37. Sjöberg, M., Dec, J., “Comparing late-cycle autoignition stability for single- and two-stage ignition fuels in HCCI engines,” *Proc. Combust. Inst.* 31: 2895-2902, 2007, doi: 10.1016/j.proci.2006.08.010.

Acknowledgments

The authors would like to thank the following people for help with this study: Kenneth St. Hilaire, Christopher Carlen, David Cicone, Alberto Garcia, and Gary Hubbard of Sandia National Laboratories for their dedicated support of the HCCI engine laboratory, and Amir Maria of Chevron, and Stephen Busch and Wei Zeng of Sandia National Laboratories for valuable suggestions on the manuscript.

Primary support for this investigation was provided by Chevron under WFO contract FI083070907-Z. The work was performed at the Combustion Research Facility, Sandia National Laboratories, Livermore, CA. Support for establishing the HCCI lab facility was provided by the US Department of Energy, Office of Vehicle Technologies, managed by Gurpreet Singh. Sandia is a multiprogram laboratory operated by the Sandia Corporation, a Lockheed Martin Company, for the US Department of Energy’s National Nuclear Security Administration under contract DE-AC04-94AL85000.

Definitions/Abbreviations

AHRR	apparent heat release rate
AKI	antiknock index
aTDC	after TDC
BDC	bottom dead center
bTDC	before TDC
CA, θ	crank angle
CA10	crank angle of the 10% burn point
CA50	crank angle of the 50% burn point
CAI	controlled auto ignition
CCG-E10	Chevron commercial gasoline containing 10 vol.% ethanol
CN	cetane number
COV	coefficient of variation
c_p	constant pressure heat capacity
CR	compression ratio
CSPd	complete stoichiometric product without water component
c_v	constant volume heat capacity
DI	direct injection
DTBP	di-tert0butyl peroxide
E10	gasoline containing 10% ethanol
EGR	exhaust gas recirculation
EHN	2-ethylhexyl nitrate
EVC	exhaust valve close
EVO	exhaust valve open
ϕ	equivalence ratio (without EGR)
ϕ_m	charge-mass equivalence ratio (including EGR)
GDI	gasoline direct injection
HCCI	homogeneous charge compression ignition
HRR	Heat-release rate
IMEP$_g$	gross indicated mean effective pressure
ITHR	intermediate temperature heat release
IVC	intake valve close
IVO	intake valve open
LTHR	low temperature heat release
MON	motor octane number
ON	octane number
PFS	partial fuel stratification
P_{in}	intake pressure
PRF	primary reference fuel
PRR	pressure rise rate
RON	research octane number
TDC	top dead center
THR	total heat release
T_{in}	intake temperature
T_{peak}	peak charge temperature
TRR	temperature rise rate